



Seismic analysis of R.C. structures using damage model and simplified modeling

Jacky Mazars¹, Stephane Grange²

¹ Professor emeritus, Grenoble Institute of Technology 3SR Laboratory, BP53 - 38000 Grenoble, France

² Professor, INSA-Lyon, Lyon University, GEOMAS, F-69621 Villeurbanne CEDEX, France

ABSTRACT

Two original characteristics distinguish the herein presented work: the strategy adopted for the finite element modeling, and the use of a newly introduced constitutive law for concrete. The aim is to be able to treat in a simplified way various structures based on column beams and bearing walls subjected to earthquakes by privileging the nonlinear 1D behavior. Applications are presented to demonstrate the pertinence of the modeling strategy used.

Keywords: Concrete structure, concrete damage model, simplified modeling, seismic vulnerability.

INTRODUCTION

When dealing with reinforced concrete (RC) structures specific attention is paid to assess (new buildings) or reassess (existing buildings) their safety level. This requires the use of high performance numerical tools that are simple enough to use, to simulate the non-linear behavior of real structures subjected to severe actions such as earthquake. This paper aims to meet this need for concrete structures by combining the use of an original material constitutive model and a simplified description of the structure.

Damage remains a major component of concrete behavior. Based on previous work [1], [2], the μ damage model [3] offers the simplest and most complete set-up possible. It implies formulating the following set of main assumptions:

- Concrete behavior is considered as the combination of elasticity and damage. The damage description is assumed to be isotropic and directly affects the stiffness evolution of the material. In the general 3D case, let \mathbf{A} be the stiffness matrix of the original material, then, the tensor stress - strain relationship is governed by:

$$\boldsymbol{\sigma} = \mathbf{A}(1 - d) : \boldsymbol{\epsilon} \quad (1)$$

- d , called the effective damage variable, characterizes the effect of damage on the stiffness activated by loading. Two principal damage modes are considered, cracking and crushing, and subsequently associated with two thermodynamic variables Y_t and Y_c , which characterize the extreme strain state reached during the loading path, respectively in the tensile part and compressive part of the strain space.

The relevance of this model has been shown in the context of classical finite element (FE) description 2D-3D, for either monotonous or cyclic loads [3].

In order to reduce the size of non-linear problems for real structures, a simplified FE description was considered for engineering purposes [4]. It is based on the use of multi-fiber beam elements for both, beams and columns. For structural walls, whose 2D-3D modeling is not always easy, it is proposed here to describe them by an in plane lattice model while recreating their bending and torsion inertia to handle out-of-plane loadings.

In such a context, it is a non-linear 1D behavior that is used for both concrete and reinforcement bars. Then it is easy to introduce, at low cost, enhancements to limit the dependence on mesh size during damage evolution as well as to take specific phenomena into account, such as steel-concrete debonding, hysteretic loops and permanent strains due to friction between crack lips and initial stresses.

CONSTITUTIVE LAWS AND NUMERICAL MODELS

Concrete model

The μ damage model is a new concrete model set up around the use of a multi-surface threshold to activate the different damage effects linked to cyclic loading, including unilateral effects (crack closure due to the reverse of the load).

Assumptions are formulated to simplify the writing, while allowing a correct description of the main non-linear effects and the 1D formulation is used in the present work.

Constitutive equations

A summary of the μ damage model is proposed below. For a more detailed presentation, see Mazars *et al.* [3], [4]. Like for a previous model, let us consider the equivalent strain concept [1]. Below, we define ε_t and ε_c as the equivalent strain for cracking and crushing, respectively (ν is the Poisson ratio):

$$\varepsilon_t = \frac{I_\varepsilon}{2(1-2\nu)} + \frac{\sqrt{J_\varepsilon}}{2(1+\nu)} ; \quad \varepsilon_c = \frac{I_\varepsilon}{5(1-2\nu)} + \frac{6\sqrt{J_\varepsilon}}{5(1+\nu)} \quad (2)$$

$$I_\varepsilon = \varepsilon_1 + \varepsilon_2 + \varepsilon_3 \quad \text{and} \quad J_\varepsilon = 0.5[(\varepsilon_1 - \varepsilon_2)^2 + (\varepsilon_2 - \varepsilon_3)^2 + (\varepsilon_3 - \varepsilon_1)^2] \quad (3)$$

Two independent loading surfaces are associated: $f_t = \varepsilon_t - Y_t$ and $f_c = \varepsilon_c - Y_c$ (4)

such that during gradual $Y_{t(c)}$ evolution, the identity $f_{t(c)} = 0$ holds, else $f_{t(c)} < 0$.

Y_t and Y_c define the equivalent strain maximum values reached on the loading path:

$$Y_t = \text{Sup}[\varepsilon_{0t}, \max \varepsilon_t] \quad \text{and} \quad Y_c = \text{Sup}[\varepsilon_{0c}, \max \varepsilon_c] \quad (5)$$

ε_{0t} and ε_{0c} are the initial thresholds of ε_t and ε_c respectively.

The effective damage d is directly correlated to the thermodynamic variables Y_t and Y_c through the driving variable Y , i.e.:

$$Y = rY_t + (1-r)Y_c, \quad \text{with} \quad r = \frac{\sum \langle \tilde{\sigma}_i \rangle_+}{\sum |\tilde{\sigma}_i|} \quad (6)$$

r is the triaxiality factor [5], which evolves within the stress space from 0, for the compressive stress zone, to 1 for the tensile stress zone; $\tilde{\sigma} = \sigma / (1-d) = \mathbf{A} : \boldsymbol{\varepsilon}$ is the "effective stress"; $\langle x \rangle_+$ and $|x|$ denote the positive part and absolute value of x , respectively. Therefore, r is damage-independent and can be determined at each calculation step without iteration, which makes this model explicit.

As was the case with the Mazars model [1], the damage evolution law is defined by:

$$d = 1 - \frac{(1-A)Y_0}{Y} - A \exp(-B(Y - Y_0)), \quad \text{where} \quad Y_0 = r\varepsilon_{0t} + (1-r)\varepsilon_{0c} \quad (7)$$

Y_0 is the initial threshold for Y . Variables A and B determine the shape of the effective damage evolution laws and subsequent constitutive laws. $[A, B]$ evolves from $[A_t, B_t]$ for the "cracking" curves to $[A_c, B_c]$ for the "crushing" curves. A_t, B_t, A_c, B_c are all material parameters directly identified from uniaxial experiments (tensile or flexural tests and compression tests).

1D version of the model

It was observed in the previous section, that the driven variable for d is Y . From equation (6) and for a uniaxial situation, it is derived that: $Y = Y_t$ for tension ($r = 1$), and $Y = Y_c$ for compression ($r = 0$).

From Equations (1) and (7), two expressions are found to describe uniaxial behavior:

- For tension: $\sigma = E(1-d_t)\varepsilon$ with $d_t = 1 - \frac{(1-A_t)Y_{0t}}{Y_t} - A_t \exp(-B_t(Y_t - Y_{0t}))$ (8)

- For compression: $\sigma = E(1-d_c)\varepsilon$ with $d_c = 1 - \frac{(1-A_c)Y_{0c}}{Y_c} - A_c \exp(-B_c(Y_c - Y_{0c}))$ (9)

where $Y_t = \text{Sup}(\varepsilon_{0t}, \max \varepsilon_t)$ with $Y_{0t} = \varepsilon_{0t} = \sigma_{0t}/E$ and where $Y_c = \text{Sup}(\varepsilon_{0c}, \max -\varepsilon_c)$ with $Y_{0c} = \varepsilon_{0c} = -\sigma_{0c}/E$.

Figure 2 shows the corresponding uniaxial response with a specific loading path, from OABE in tension to OCDF in compression, while highlighting the range of evolution in stiffness due to crack opening and closure (i.e. the unilateral effect).

Modeling strategies

Multi-fiber beam elements

To decrease the number of degrees of freedom, 3D Timoshenko multi-fiber beam elements have been used [6]. This beam description generates kinematic constraints to ensure respecting both, the continuity of displacement between two elements

and all plane sections. However, this leads to generate only the need of 1D constitutive laws. In this context, nonlinear fibers are associated with the 1D μ damage model for concrete and with an elasto-plastic model for rebar.

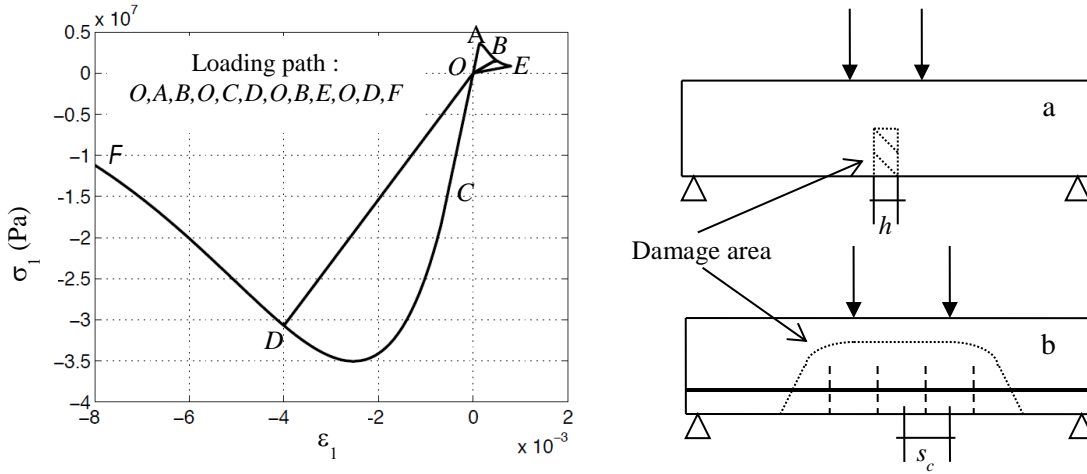


Figure 1(on the left) - Tension-compression loading path exhibiting the unilateral effect.

Figure 2 (on the right) - Localization processes in a multi-fiber beam description; a) plain concrete: damage is localized in a band of elements (size h); and b) reinforced concrete: damage is distributed along the cracking zone (s_c is the crack spacing)

Concrete exhibits softening, which in turn leads to strain localization and results can be dependent on element size. Strain localization is a major concern in maintaining the objectivity of finite element calculations. Hillerborg stipulated that the energy dissipated at failure in a unit concrete volume must be equal to the fracture energy G_f [7]. In classical 2D-3D calculations (FE), localization takes place within a band of elements, and the material parameters must be calibrated with the size h of these elements (Fig. 2a). In a recent paper [4], it was demonstrated that for reinforced concrete members discretize using Timoshenko multi-fiber beams elements (MF), except in pure tension and for a low amount of rebar, no localization is present. Concrete damage spreads and diffuses in the highest tension area (Fig. 2b).

As shown Fig. 2b, in the absence of localization, the damage-cracking processes for one crack are distributed on both sides of the crack over a volume defined by the distance s_c between two cracks. Therefore, the concept of crack band cannot be applied and the calculation must be calibrated so that the fracture energy is consumed in a s_c wide area, leading us to write:

$$G_f = s_c \int \sigma d\epsilon \quad \text{with:} \quad s_c \int_{MF} \sigma d\epsilon = h \int_{FE} \sigma d\epsilon \quad (10)$$

Lattice model for structural walls: Equivalent Reinforced Concrete (ERC)

Figure 3 shows the principle of the equivalent reinforced concrete method (ERC). We start from a representative volume of the wall at the intersection of the 2 reinforcement networks (vertical and horizontal), it includes an elementary volume of concrete, represented by a rectangular assembly of 6 bars and the related rebar represented by a rectangle of 4 bars coupled to the previous one at the level of the nodes (see [8] for more details). The bars being articulated have a uniaxial behavior. Those relating to concrete will have an elasto-damageable behavior and those relating to steel will have an elasto-plastic behavior, the same as those used in finite element calculations, except that, being uniaxial, it is easier to enrich them to take into account the particularities of the problem treated (hysteresis and permanent strains of the concrete behavior for example).

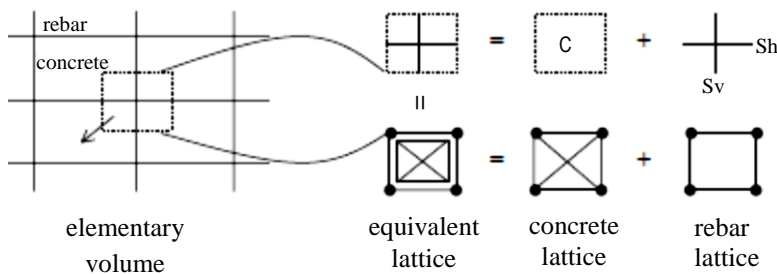


Figure 3- Equivalent Reinforced Concrete modeling [8].

On the basis of energy equivalence between the homogeneous body and the network of bars substituted for it, Hrennikoff [9] determined the cross-section of the concrete lattice for an elastic problem. The real section is taken for the rebar lattice. Note that this type of discretization imposes an overall Poisson coefficient equal to 1/3.

Constitutive model enhancement

In the present modeling strategy (multi-fiber beam and ERC wall), the behavior of each fiber is uniaxial. Then it is possible to improve them easily to take into account various phenomena. In this framework and to improve concrete and steel cyclic behavior, an enhanced 1D version of both models can be proposed.

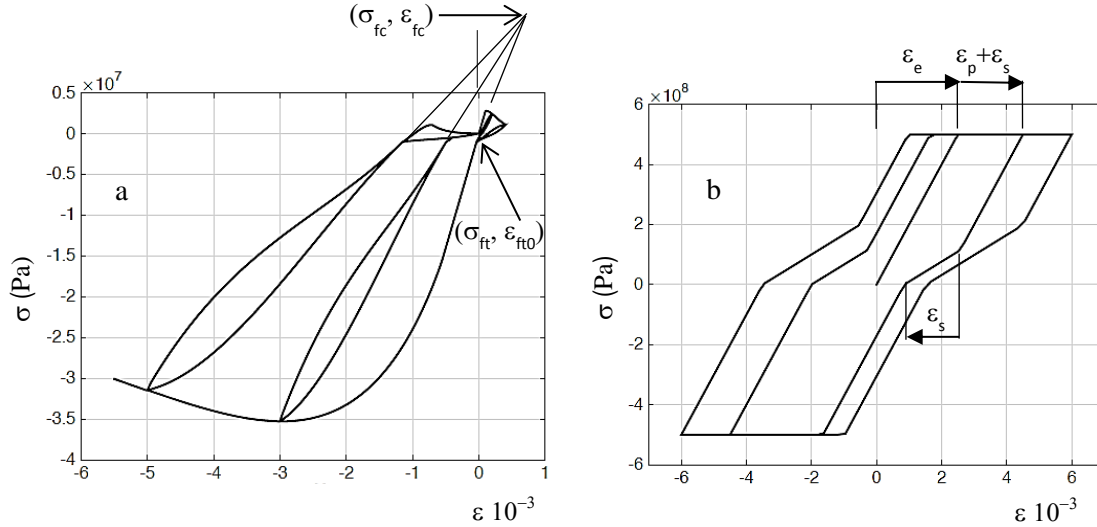


Figure 4 – Enhanced constitutive 1D models: a) concrete curve including hysteretic loops and permanent strain; b) rebar-concrete bond curve obtained by introducing a sliding stage into the global steel fiber behavior.

To improve replication of the concrete cyclic behavior, we have upgraded the 1D version of the μ damage model presented before, by introducing a hysteretic loop as well as the permanent strain generated from friction between the crack lips and the release of initial stresses (Fig. 4a).

Related to rebar behavior, it is widely acknowledged that debonding between concrete and rebar occurs at large deformations. This phenomenon is especially sensitive whenever cracks open and steel yields. In a fiber beam description, given that no interaction is taking place between the fibers except at their ends and that the damage-fracture processes are distributed, debonding cannot be reproduced. This point leads to overestimating the plastic strain [4]. One way to introduce bond degradation and the relative sliding of rebar over concrete in a multi-fiber beam description is to split the total strain in the steel fiber into two parts: a first part associated with the proper strain of the steel ($\epsilon_e + \epsilon_p$), and the second part related to the sliding strain (ϵ_s) occurring at the steel-concrete interface (see Fig. 4b). And, due to the crack closure, ϵ_s gradually vanishes and reaches 0 when the strain sign changes.

APPLICATIONS

The simulations presented in this paper have been made on the platform *ATLAS* developed at INSA Lyon [10] for internal numerical developments and initially inspired by the philosophy of data entry of FEDEASLAB [11].

Shear wall SAFE

The “SAFE” test program has been performed on the reaction wall at JRC Ispra (Italy) and was sponsored by EDF. Schematically the wall to be modeled is given figure 5 [12]. The choice is to consider only the wall subdomain in a non-linear lattice model (ERC model), integrating the current reinforcements (HA8 vertical and HA10 horizontal with a spacing of 12.5cm). Both, left and right orthogonal reinforcing walls, are represented by a multi-fiber beam (0.16x0.8m) elasto-damageable, including the actual vertical reinforcements (20 HA12). Elastic and highly rigid beams (section area # 1m²) are used at the top and the bottom of the walls to apply correctly the boundary conditions.

These tests were conducted on a reaction wall by a "pseudo dynamic" procedure. The dynamic equilibrium of the structure involves masses and acceleration increments and the measured resisting force provides the displacement increments to be applied to the wall at each time step. Since the data provide the evolution in time of the applied displacement, we decided to

simulate the loading by directly imposing the proposed displacement steps on the structure. As time becomes a fictitious time, inertia is not involved and the loading becomes a cyclic loading with variable intensity as in the pseudo-dynamic test.

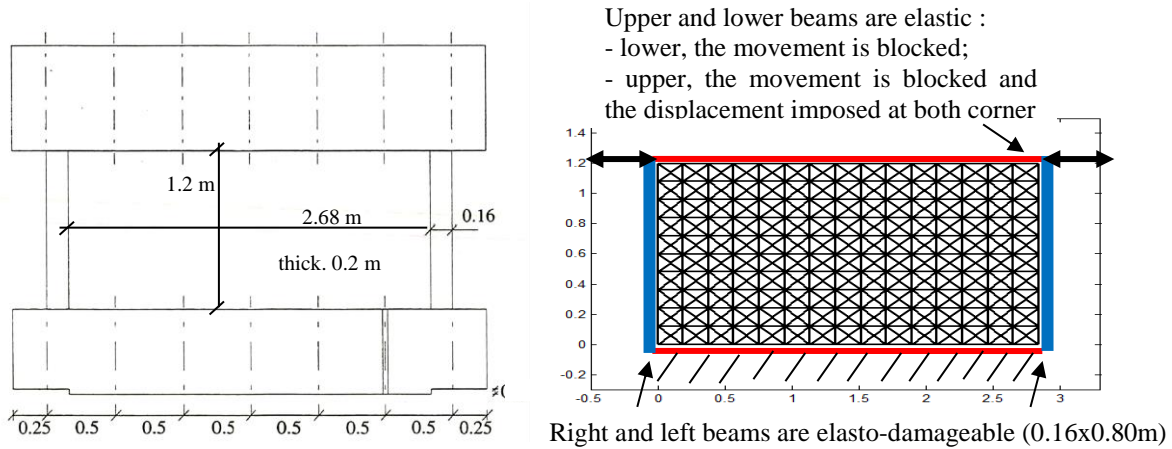


Figure 5- Scheme of the wall to be modeled and the selected discretization.

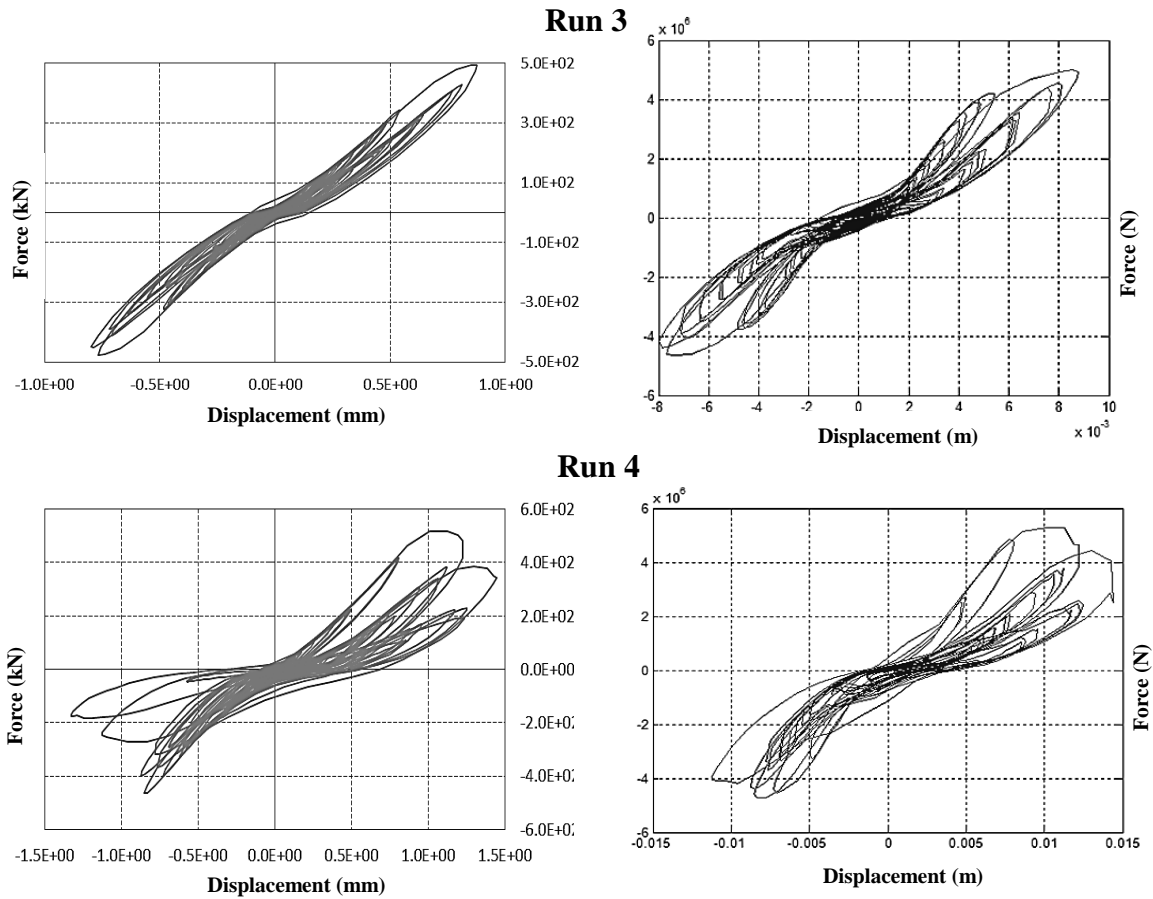


Figure 6- Overall force-displacement behavior of the SAFE wall in cyclic loading (Run 3 and 4). On the left, experimental response, on the right, numerical response.

Figure 6 shows, for the most intense cycles (run n°3 and 4), the force - displacement comparison between the test results (left) and the numerical results (right). The numerical results are quite relevant to those given by the tests, including for the run n° 4 which leads to structural failure. In the context of an organized benchmark on the subject, they appear among the best results.

SMART shaking table test

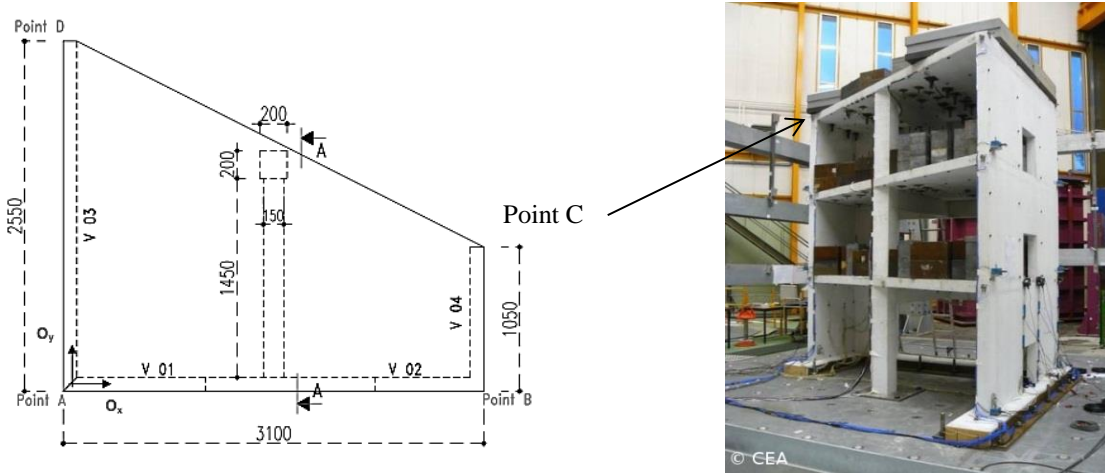


Figure 7- SMART mock-up[13]. Drawing related to a storey of the structure (left). General view of the experiment (right).

This test, sponsored by EDF, was performed on the shaking table at CEA Saclay, France. The mock-up (Fig. 7) is a trapezoidal three-storeys structure representative of a real building at scale 1/4, mainly composed of structural walls, with in addition, one column and three beams (under each slab). Herein, both, the columns and the beams have been modeled by means of Timoshenko multi-fiber beam elements whilst the slabs have been modeled through elastic shell elements. The ERC approach [8] has been used for the modeling of the structural walls. Furthermore, in order to be suitable for the modeling of the three-dimensional SMART structure, the ERC modeling necessitates to be completed by vertical beam-layer with no mass and no stiffness, but giving out-of-plane inertias (see Fig. 8).

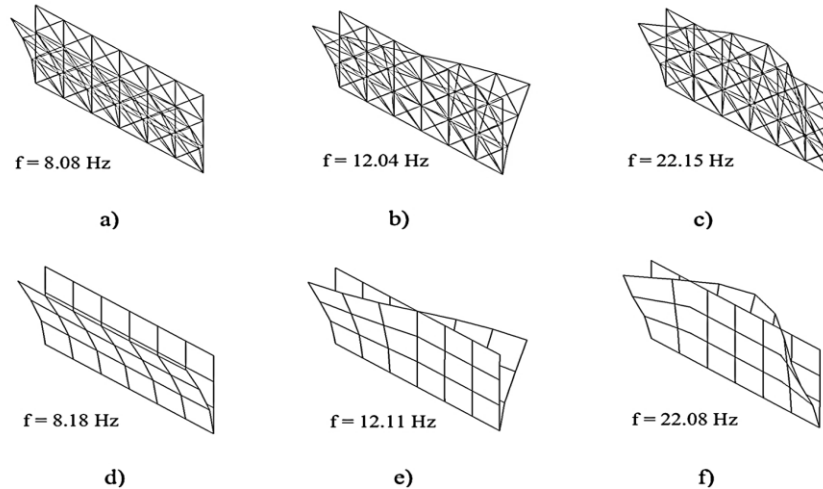


Figure 8 - Tuning of the out-of-plane stiffness in the enriched-ERC modeling. The enriched-ERC model (a, b, c) have same dimensions, mass and mesh-size of the shell model (d, e, f). The moments of inertia (J_{xx} and J_{yy}) and the torsion inertia moment (JT) of the added vertical beam-layer are tuned in order to reproduce (a, b, c) the first three modal frequencies and shapes of the “reference” shell model (d, e, f). Reproduced from [14].

Finally, the mass of the structure is distributed on the elements (beams, column, slabs and walls) whilst the additional masses (located on the upper level) have been explicitly modeled through massive (3D) elements. For the steel reinforcement bars, a classical elasto-plastic constitutive relation has been selected. The damage-based constitutive law (μ model) chosen to represent concrete behavior for both, beams, columns (multi-fiber beam modeled) and shear walls (lattice modeled), can take into account the decrease in stiffness due to cracking, as well as the stiffness recovery that occurs at crack closure (Figure 4b).

Predicted response

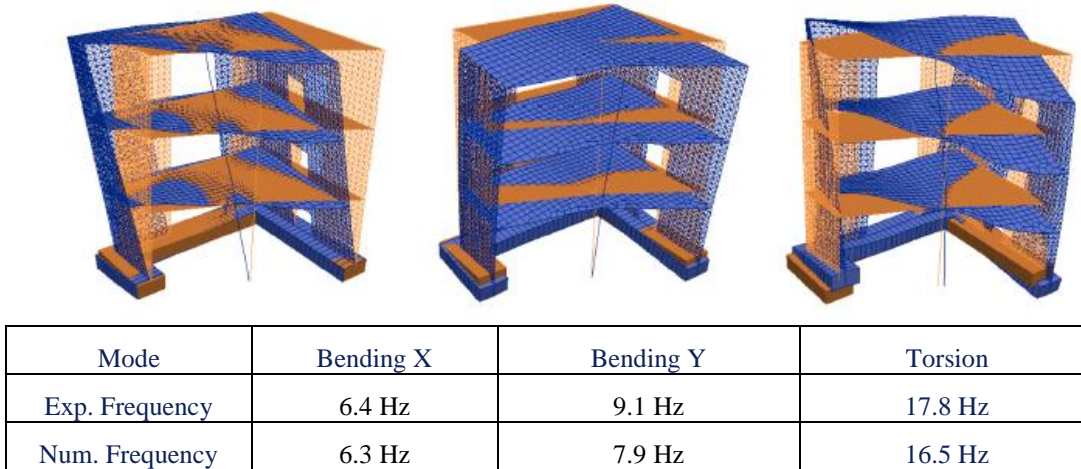


Figure 9- Vibration modes of the mock-up on the shaking table (for better clarity, the shaking table and the additional masses are not visualized): a) bending X-direction; b) bending Y-direction; c) torsion. Reproduced from [14].

The mock-up is loaded in a bidirectional way and the loading program included 3 main phases: 1/ artificial earthquake respecting the design spectrum ($p_{ga} = 0.22g$); 2/ Northridge natural earthquake ($p_{ga} = 1.1g$) and 3/Northridge replica.

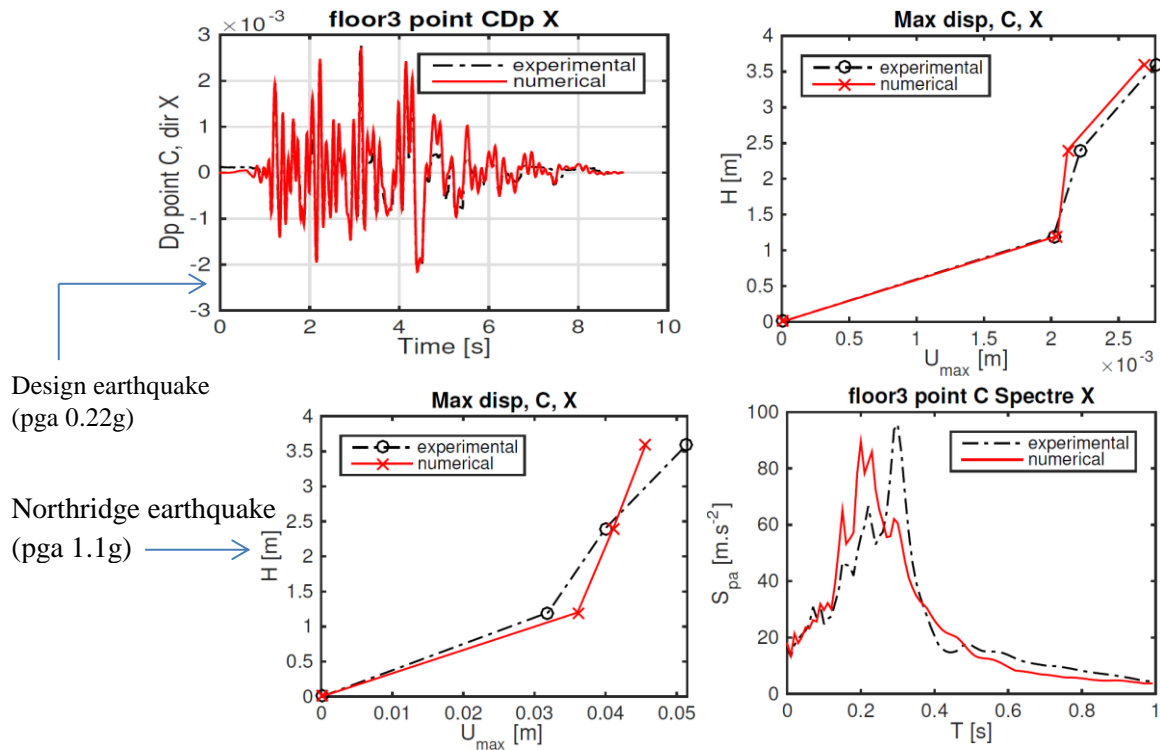


Figure 10- Experimental vs. numerical comparison - RUN 9, design earthquake: a) displacement history at point C, third floor, X-direction; b) maximum displacement at each floor, point C, X-direction - RUN 19 (Northridge earthquake): c) maximum displacement at each floor, point C, X-direction, and d) acceleration spectrum at point C, third floor, X-direction.

The figures 9 and 10 report a comparison of numerical vs. experimental results in terms of modes and displacements. Figure 9 represents the first three vibration modes of the structure issued of modal analysis; the associated frequency values are reported in the figure.

Among the several runs performed, figure 10 presents some displacement results on 2 specific ones:

- Run n°9 (design level), for which the X experimental and numerical displacement history at point C - 3rd floor and the maximum values at this point on each floor, are compared.
- Run n°19 (Northridge signal), for which experimental and numerical maximum values of the X-displacement at point C on each floor, and the acceleration spectrum at point C, 3rd floor, direction X, are compared.

Overall, these results are good, in any case as good as those shown during the 2013 SMART benchmark with much more refined discretization (2D-3D) [13].

CONCLUSIONS

The aim of this work is to be able to treat in a simplified way of various structures subjected to earthquakes based on column beams and bearing walls. This is done by focusing on two main aspects: the strategy adopted for the finite element modeling and the relevance of constitutive models.

To model slender element such as beam or column Timoshenko multi-fiber beams are privileged and for bearing walls a lattice based model is proposed using the equivalent reinforced concrete model (ERC). The main interest of this type of modeling strategies (multi-fiber beams and ERC model) is that, being based on uniaxial behavior, it makes the application to non-linear calculation easy and robust. This is not always the case for 2D or 3D damage or smeared crack approaches, particularly under shear, where localization phenomena can compromise the convergence and the robustness.

The non-linear concrete constitutive model used is the 1D version of the μ damage model well adapted to describe cyclic and dynamic loading. In both descriptions, multi-fiber beams and ERC model for concrete elements and bar elements for rebar, a 1D classical elasto-plastic model can be used.

The applications proposed are on a shear wall (SAFE program performed on the ELSA reaction wall at JRC Ispra) and on a mock-up representative of a power plant building, tested on the Azalée shaking table at CEA Saclay (EDF SMART program). Comparative calculation-experiment results show the relevance of the modeling, which is also reliable and inexpensive.

ACKNOWLEDGMENTS

The authors would like to thank Dr. M. de Biaso for his valuable assistance in providing the results performed in the framework of the SMART 2013 benchmark [14].

REFERENCES

- [1] Mazars J., 1986. A description of micro and macroscale damage of concrete structure. *Engineering Fracture Mechanics*, Vol25, p729-737.
- [2] Pontiroli C., Rouquand A., Mazars J., 2010. Predicting concrete behaviour from quasi-static loading to hypervelocity impact. *European Journal of Environmental and Civil Engineering*, Vol. 14, N° 6-7, pp. 703-727.
- [3] Mazars J., Hamon F., Grange S., 2015, A new 3D damage model for concrete under monotonic, cyclic and dynamic loading, *Materials and Structures*, 48, 3779–3793
- [4] Mazars J., Grange S., 2015. Modeling of Reinforced Concrete Structural members for Engineering Purposes, *Computers and Concrete*, 16(5) 683-701.
- [5] Lee J., Fenves G.L., 1998, Plastic-Damage Model for Cyclic Loading of Concrete Structures, *J. Eng. Mech.* 124, 892.
- [6] Kotronis, P. and Mazars, J., 2005. Simplified modelling strategies to simulate the dynamic behaviour of r/c walls. *Journal of Earthquake Engineering*, 9(2):285–306.
- [7] Hillerborg A., Modeer M., Petersson P.E., 1976. Analysis of crack formation and growth in concrete by means of fracture mechanics and finite elements, *Cement and Concrete Research*, Vol.6, pp773-782.
- [8] Kotronis P., Mazars J., Davenne L., 2003. The equivalent reinforced concrete model for simulating the behavior of shear walls under dynamic loading. *Engineering Fracture Mechanics*, Elsevier, 70 (7-8), pp.1085-1097.
- [9] Hrennikoff A., 1941. Solution of Problems of Elasticity by the Frame-Work Method, *ASME J. Appl. Mech.* 8, 619–715.
- [10] Grange S., 2015. ATL4S - A Tool and Language for Simplified Structural Solution Strategy - Intern. report, GEOMAS.
- [11] Filippou, F. C. and M. Constantinides (2004). "FEDEASLab getting started guide and simulation examples." *NEESgrid Report 22: 2004-2005*.
- [12] Labbé P., Pegon P., Molina J., Gallois C., Chauvel D., 2015. The SAFE Experimental Research on the Frequency Dependence of Shear Wall Seismic Design Margins, *Journal of Earthquake Engineering*, pp. 101-128
- [13] Richard B. et al., 2014. SMART 2013: overview, synthesis and lessons learnt from the International Benchmark, *SMART 2013 workshop*, Paris - Saclay, France.
- [14] De Biasio M. et al., 2014. Modeling structural-wall buildings through an Enriched E R C method and a new Damage-based Concrete constitutive law: the SMART2013 case study. *SMART 2013 workshop*, Paris-Saclay, France.